An ab Initio Study of Hydrogen Bonding Effects on the ^{15}N and ^{1}H Chemical Shielding Tensors in the Watson−Crick Base Pairs

Jiří Czernek*

Institute of Macromolecular Chemistry, Academy of Sciences of the Czech Republic, Heyrovsky Sq. 2, 162 06 Praha 6, Czech Republic

Received: September 25, 2000; In Final Form: December 27, 2000

Density functional theory is applied to explore changes upon hydrogen bonding in the ^{15}N and ^{1}H nuclear magnetic resonance (NMR) chemical shielding tensors of the imino group in the Watson−Crick nucleic acid base pairs. The dependence of results on the quantum chemical method used, on the basis set superposition error, and on the effect of the relaxation of the base pair geometry with changing hydrogen bond length is addressed. The systematic variation with changing separation between bases in calculated shielding data and resulting auto- and cross-corelation chemical shift anisotropy parameters is documented. Possible implications for NMR studies of the dynamics of $^{15}N-^{1}H$ bond vectors and for transverse relaxation-optimized spectroscopy experiments on imino protons are discussed.

Introduction

Modern nuclear spin relaxation measurements are capable of probing a vast time range of molecular motions.[1] As a result, the study of biopolymer mobility in solution using NMR becomes increasingly important in unraveling correlations between the function and dynamics of macromolecules.[2] When applied to nucleic acids, relaxation studies of internal motions have primarily focused on the ^{15}N isotope of the imino group.[3] Structurally, imino groups are important hydrogen-bond donors in nucleic acids. In the Watson−Crick base pairs, they form such bonds with the N3 nitrogen of cytosine (in the guanine−cytosine base pairs) and with the N1 nitrogen of adenine (in the thymine−adenine DNA base pairs and in the uracil−adenine RNA base pairs);[4] the separation between imino nitrogen and the N3/N1 cytosine/adenine acceptor will be denoted here as rN···N (see Figure 1). For a reliable interpretation of ^{15}N relaxation data, the knowledge of both imino nitrogen and imino proton chemical shielding tensors becomes crucial. Very recently, these tensors, in contrast to what has been sometimes assumed, have been shown not to be axially symmetric with respect to the imino $^{15}N-^{1}H$ bond vector.[5,6,7] Moreover, from the first systematic investigation of changes in shielding tensors with varying rN···N in the guanine−cytosine pair,[7] site-specific variations in principle elements and directional cosines of ^{15}N and ^{1}H shielding tensors have been inferred. The resulting systematic errors in parameters of molecular motion based on autocorrelation rates have been analyzed for imino nitrogens of guanine residues in nucleic acids. As recently proposed transverse relaxation-optimized spectroscopy (TROSY)[8] is the focus of increasing attention in the NMR of nucleic acids,[9] simulations of TROSY effects for guanine imino nitrogen have been carried out in the communication[7] as well. Clearly, an extension of this study to remaining Watson−Crick base pairs, together with an assessment of the efficiency of TROSY experiments for imino protons in nucleic acids, are of utmost interest.

* Present address: Gustav H. Carlson School of Chemistry, Clark University, 950 Main St., Worcester, MA 01610-1477. Fax: +1-508-793-8861. Phone: +1-508-793-7112. E-mail: george@nmr.clarku.edu.

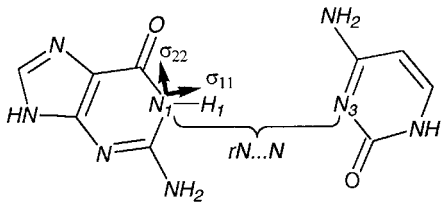

Figure 1. Definition of the rN···N separation in the guanine−cytosine base pair and the orientation of the principal axis system of the ^{15}N chemical shielding tensor of the N1 nucleus of guanine in the frame of reference of the base pair (σ_{33} is perpendicular to the page).

In this report, particular attention has been paid to the technical details of chemical shielding calculations (for a recent review of ab initio calculations of NMR parameters, see ref 10). Consequently, the following topics will be addressed:

(i) Presently, for chemical shielding tensors to be calculated with the inclusion of electron correlation, only density functional theory (DFT)[11]-based methodologies are of practical use when systems comprising more than 20 non-hydrogen atoms are in question. Of them, the B3LYP-GIAO[12] and the SOS-DFPT-IGLO[13,14] approaches seem to be the leaders.[15] Do shielding tensors and, as a consequence, relaxation properties of imino nuclei as predicted by these alternative approaches differ significantly?

(ii) Although large basis sets have been used, they are obviously finite, and thus, computed shielding tensors are, in principle, affected by the basis set superposition error (BSSE).[16] Should calculated shielding parameters be BSSE-corrected?

(iii) In general, modification of the rN···N distance is accompanied by changes in remaining geometrical parameters of the base pair. How important is this effect for derived relaxation parameters?

On the basis of solutions to the methodological questions, the systematic variation in ab initio shielding data in response to the hydrogen bond length will be discussed. Chemically and spectroscopically relevant conclusions will be drawn mainly concerning the following:

(iv) Differences in ^{15}N and ^{1}H shielding tensors between thymine and uracil, respectively, when hydrogen-bonded to adenine.

10.1021/jp003471g CCC: $20.00
Published on Web 02/02/2001

(v) Changes in shielding of the ^{15}N and ^{1}H atoms of imino group when located on guanine and a pyrimidine base, respectively, when *r*N···N is modified to mimic different sites of nucleic acids.
(vi) Finally, ab initio predicted shielding tensors will be employed in simulations of spin−spin relaxation rates of imino protons for two approaches of relaxation control, i.e., single-quantum coherence (SQ) experiments[17,18] and the TROSY scheme. The data obtained by these simulations will be shown to be useful in guiding experimental work on the structure and dynamics of nucleic acids.

Theory and Computations

Geometries. The proper description of geometries of hydrogen-bonded nucleic acid bases is a demanding task.[19] In the study of the guanine−cytosine pair,[7] coordinates from a deliberately selected crystal structure were employed. In the present work, geometry optimizations with the inclusion of electron correlation were carried out instead. Since calculations on the MBPT(2)[20] (or higher) level with a reasonably large basis set would be extremely demanding, DFT was employed. In a thorough investigation[21] of vibrational spectra of hydrogen-bonded bases, the B3PW91/6-311G approach was adopted. It was pointed out to the author[22] that the B3PW91 functional tended to give hydrogen bond lengths that were too short relative to the results of optimizations with the B3LYP (Becke's three parameter exchange[23] and Lee, Yang, Parr correlation[24]) functional. This was confirmed (values not shown) for the cytosine dimer, for which extensive MBPT(2) data were reported as well.[25] Consequently, the B3LYP/6-311G approach was used. HF/6-31G** geometries of the guanine−cytosine (GC), adenine−thymine (AT), and adenine−uracil (AU) base pairs as obtained from an author of ref 25 served as an initial guess for full geometry optimizations using the Gaussian94[26] suite of programs with default settings. Located stationary points were verified to be minima by calculations of harmonic vibrational frequencies (all real for each structure). From these minima, the structures with *r*N···N separations between 2.65 and 3.50 Å (see Tables 4−6 and 8−10) were prepared by translation along the direction of respective imino nitrogen−N3/N1 axis. To study an implicit influence of changes in geometrical parameters other than *r*N···N on shielding tensors, we carried out partial optimizations at the B3LYP/6-311G level for the AT pair by freezing the *r*N···N distance at its lowest (2.65 Å) and highest (3.50 Å) values considered here and by relaxing remaining internal coordinates. The coordinates of the equilibrium and the relaxed geometries of the AT pair are available as Supporting Information (Table 1S).

NMR Chemical Shielding and Relaxation. A thorough discussion of this topic was most recently given in ref 7. Consequently, only a brief summary follows here.

The chemical shielding tensor, σ, is a tensor of rank 2. ${\sigma_{11}}^{A} \leq {\sigma_{22}}^{A} \leq {\sigma_{33}}^{A}$ are the components of the diagonalized shielding tensor of an atom A. ${\sigma_{iso}}^{A} = ({\sigma_{11}}^{A} + {\sigma_{22}}^{A} + {\sigma_{33}}^{A})/3$ is the isotropic chemical shielding, and $\delta^{A} = \sigma_{ref} - {\sigma_{iso}}^{A}$ is the isotropic chemical shift of an atom A, where σ_{ref} is the isotropic shielding of a (NMR-active) nucleus A in a reference compound.

The chemical shift anisotropy (CSA) interaction between the applied magnetic field $\mathbf{B_0}$ and the nuclear magnetic moments is often a significant relaxation mechanism. CSA autocorrelation processes[27] for an axially symmetric shielding tensor depend on the parameter termed CSA

$$\mathrm{CSA} = \sigma_{\parallel} - \sigma_{\perp} \tag{1}$$

where $\sigma_{\parallel}$ and $\sigma_{\perp}$ are the chemical shieldings of the nucleus under study when $\mathbf{B_0}$ is parallel and orthogonal, respectively, to the axis of symmetry of the shielding tensor. For a nonsymmetric shielding tensor, parameters $\Delta\sigma$ and $\Delta\eta$ (the asymmetry factor) can be used to describe CSA autocorrelation. Here, $\Delta\sigma$ of an imino nitrogen, $\Delta\sigma^{N}$, is defined as

$$\Delta\sigma^{N} = {\sigma_{11}}^{N} - ({\sigma_{22}}^{N} + {\sigma_{33}}^{N})/2 \tag{2a}$$

and $\Delta\sigma$ of an imino proton, $\Delta\sigma^{H}$, as

$$\Delta\sigma^{H} = {\sigma_{33}}^{H} - ({\sigma_{11}}^{H} + {\sigma_{22}}^{H})/2 \tag{2b}$$

on the basis of the observations (cf. Discussion) that (a) the principal axis of ${\sigma_{11}}^{N}$ is close to $\sigma_{\parallel}$ of imino ^{15}N shielding tensors and (b) the principal axis of ${\sigma_{33}}^{H}$ is close to being collinear with the imino ^{1}H−^{15}N bond vector. Accordingly, the asymmetry factors are defined as

$$\Delta\eta^{N} = ({\sigma_{22}}^{N} - {\sigma_{33}}^{N})/({\sigma_{11}}^{N} - {\sigma_{iso}}^{N}) \tag{3a}$$

and

$$\Delta\eta^{H} = ({\sigma_{22}}^{H} - {\sigma_{11}}^{H})/({\sigma_{33}}^{H} - {\sigma_{iso}}^{H}) \tag{3}$$

The chemical shift anisotropy contribution to autocorrelation, $\mathrm{CSA_a}$, is then given by

$$\mathrm{CSA_a} = \Delta\sigma\,(1 + \Delta\eta^{2}/3)^{1/2} \tag{4}$$

It is stressed that the definitions 2a,b and 3a,b are invoked only for convenience, as CSA autocorrelation properties can be alternatively defined using the effective $\Delta\sigma$, $\Delta\sigma_{eff}$[28]

$$\Delta\sigma_{eff} = ({\sigma_{11}}^{2} + {\sigma_{22}}^{2} + {\sigma_{33}}^{2} - \sigma_{11}\sigma_{22} - \sigma_{11}\sigma_{33} - \sigma_{22}\sigma_{33})^{1/2} \tag{5}$$

which is equivalent to $\mathrm{CSA_a}$ in the sense that $|\mathrm{CSA_a}| = \Delta\sigma_{eff}$ (see ref 7 for discussion).

The cross-correlation CSA processes[29] depend, in addition, on the principal values of the shielding tensor and also on the orientation of the shielding tensor with respect to the internuclear axis. In the case of a nonsymmetric tensor, cross-correlated relaxation rates depend on the parameter Γ

$$\Gamma = \sigma_{11}P_2(\cos\theta_1) + \sigma_{22}P_2(\cos\theta_2) + \sigma_{33}P_2(\cos\theta_3) \tag{6}$$

where θ_i is the angle between the *i*-th component of the shielding tensor in its principal axis system and the internuclear (^{15}N−^{1}H imino, e.g.) vector and $P_2(x) = (3x^2 - 1)/2$.

Shielding Tensors. SOS-DFPT-IGLO shielding tensors were obtained with the deMon-MASTER-CS code,[30,31] which implements sum-over-states density functional (Rayleigh−Schrödinger) perturbation theory with the IGLO[32] gauge choice. The Perdew−Wang-91 exchange-correlation potential,[33,34] the FINE angular integration grid with 32 radial shells,[14] and the approximation Loc. 1 SOS-DFPT[13,14] were used. The molecular orbitals were localized by the method of Boys.[35] To obtain more precise molecular orbital coefficients and one-electron energies after reaching convergence during SCF iterations, we performed one extra iteration without fitting the exchange-correlation potential and using an enlarged grid.[14] The IGLO−III basis set of Kutzelnigg et al.[32] was employed. IGLO−III is a relatively large basis set, roughly of "quadruple-ζ" quality (the contraction pattern (6)/[3,3*1] with two sets of polarization functions for hydrogen and (11;7)/[5,6*1;2,5*1] with two *d* sets for first-

row atoms). Its use resulted in the application of 813, 756, and 803 basis functions for the AT, AU, and GC base pairs, respectively. To account for the basis set dependence of shielding tensors, we used a huge JMN2 basis set[14] (uncontracted IGLO−III with two additional sets of polarization functions) together with the same protocol as described above in selected calculations of the AT pair (Tables 1 and 2). The number of basis functions increased to 1262. These calculations will be abbreviated as IGLO/III and IGLO/JMN2, respectively.

To check the dependence of shielding tensors in the AT pair on the method used, we employed the B3LYP-GIAO approach as implemented in the Gaussian94[26] suite of programs. In this scheme, the GIAO[36,37] method is used to overcome the gauge problem, and coupled-perturbed Kohn−Sham equations with the presence of Hartree−Fock exchange terms are solved.[12] The basis set used was the TZ2P by Schäfer et al.[38] It is a triple-ζ basis set with two polarization functions (the contraction pattern (5)/[3] for hydrogen and (10;6)/[6;3] for the rest of atoms; 574 basis functions). The resulting approach will be referred to as GIAO/TZ2P.

In agreement with the previous work[39] on biological systems of similar size to base pairs, anhydrodeoxythymidines, considerable time savings can be achieved by the application of the IGLO/III method as compared to the GIAO/TZ2P method. For example, typical CPU times on the same SGI Power Challenge computer with R10000 processors for the AT pair were 8 and 50 h accordingly.

To determine the extent of BSSE in IGLO/III calculations, we obtained counterpoise (CP) corrections of Boys and Bernardi[40] to selected σ_{iso}, σ_{ii}, and θ_i values of the AT pair with rN···N = 2.65 Å (see Table 3 and Discussion). In this approach, tensor parameters were calculated for thymine in the presence of the basis functions of adenine (without its electrons or nuclei).

Simulations of Relaxation Rates. The relaxation rate constants for the slowly relaxing (TROSY) component of the imino ^{1}H−^{15}N doublet, R_2^{TR}, and for the imino ^{1}H single quantum coherence, R_2^{SQ}, were calculated according to the following equations:[9]

$$R_2^{TR} = d_{HN}^2/8[4J(0) + J(\omega_N - \omega_H) + 3J(\omega_H) + 3J(\omega_N) + 6J(\omega_N + \omega_H)] + (c_H^2/6)[4J(0) + 3J(\omega_H)] + (c_N^2/2)3J(\omega_N) + 1/(2\sqrt{3})g_H d_{HN}[4J(0) + 3J(\omega_H)] + \sum_{H'} d_{HH'}^2/8[J(0) + 3J(\omega_H) + 6J(2\omega_H)] \quad (7)$$

$$R_2^{SQ} = d_{HN}^2/8[4J(0) + J(\omega_N - \omega_H) + 3J(\omega_H) + 3J(\omega_N) + 6J(\omega_N + \omega_H)] + (c_H^2/6)[4J(0) + 3J(\omega_H)] + (c_N^2/2)3J(\omega_N) + \sum_{H'} d_{HH'}^2/8[J(0) + 3J(\omega_H) + 6J(2\omega_H)] \quad (8)$$

where

$$d_{HN} = \gamma_H \gamma_N h\mu_0/(8\pi^2 r_{HN}^3) \quad (9)$$

$$d_{HH'} = \gamma_H^2 h\mu_0/(8\pi^2 r_{HH'}^3) \quad (10)$$

$$c_H = \omega_H CSA_a(H)/3 \quad (11)$$

$$c_N = \omega_N CSA_a(N)/3 \quad (12)$$

$$g_H = \omega_H \Gamma_H/\sqrt{3} \quad (13)$$

where J is the power spectral density function,[41] μ_0 is the permittivity of free space, h is Planck's constant, γ_H and γ_N are the gyromagnetic ratios of the spins ^{1}H and ^{15}N, respectively,

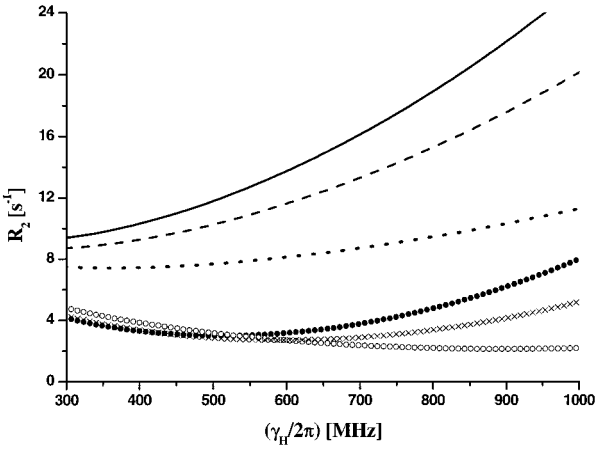

Figure 2. Transverse relaxation rate dependence on the spectrometer strength theoretically predicted for the imino proton in the adenine−thymine base pair. Straight lines: single quantum coherence for a molecule with short (solid line; rN···N = 2.65 Å), typical (dashed line; rN···N = 2.79 Å), and long (dotted line; rN···N = 3.25 Å) hydrogen bonds. Symbols: the slowly relaxing (TROSY) component of the HN doublet for rN···N values of 2.65 Å (solid circles), 2.79 Å (crosses), and 3.25 Å (open circles). See the text for details of simulations.

r_{HN} is the ^{1}H−^{15}N internuclear distance, $r_{HH'}$ are the interproton distances considered (vide infra), ω_H and ω_N are the Larmor frequencies of ^{1}H and ^{15}N, respectively, and the chemical shift anisotropies CSA_a and Γ were calculated from eqs 4 and 6, respectively. As the H′ protons in eq 10, only the ^{1}H nuclei with distances from the imino proton smaller than 3.0 Å (data not shown) in the B3LYP/6-311G geometry were taken. Namely, the H2(A) and one of the amino protons were considered in simulations of the AT pair. In the case of the GC pair, one amino proton of guanine and one amino proton of cytosine were investigated. As the values of the r_{HN} separation, 1.0550 and 1.0363 Å were used for the AT and the GC pair, respectively (see Discussion). The dynamic model considered in the simulations is that derived using the Lipari−Szabo approach.[42,43] The analytical spectral density function for this model is

$$J(\omega) = 2/5[S^2\tau_m/(1 + \omega^2\tau_m^2) + (1 - S^2)\tau/(1 + \omega^2\tau^2)] \quad (13)$$

with

$$1/\tau = 1/\tau_m + 1/\tau_e \quad (14)$$

where τ_m is the rotational correlation time, τ_e is the effective internal correlation time, and S^2 is the generalized order parameter that describes the balance between contributions to $J(\omega)$ due to overall rotation and internal motion. As the values of correlation times, the estimates[9] for the ATP-binding RNA aptamer[44] at 298 K, i.e., $\tau_m = 8 \times 10^{-9}$ s and $\tau = 8 \times 10^{-12}$ s, were taken. The effect of flexibility of a molecule was examined by repeating calculations for several S^2 values from the interval $\langle 0.25,1.0 \rangle$, i.e., by modeling highly flexible to rigid residues.

Taking into account the above-mentioned parameters, the relaxation rate constants as function of B_0 (see Figures 2 and 3) and their derivatives dR_2/dB_0 were studied using a routine in Maple V.[45]

Results and Discussion

Methodological Aspects. IGLO/III, IGLO/JMN2, and GIAO/TZ2P results for the AT pair in several rN···N separations are

TABLE 1: Chemical Shift Anisotropies of the N3 Atom of Thymine as Predicted Using Different Approaches[a,b]

	2.65 Å		2.79 Å		3.50 Å		∞	
approach	CSA_a [ppm]	Γ [ppm]	CSA_a [ppm]	Γ [ppm]	CSA_a [ppm]	Γ [ppm]	CSA_a [ppm]	Γ [ppm]
IGLO/III	−134.3	−85.9	−123.6	−89.0	−99.3	−92.6	−93.7	−91.7
	(−133.9)	(−84.6)			(−106.6)	(−98.5)	(−101.5)	(−98.8)
IGLO/JMN2	−136.1	−87.2	−129.3	−92.0	−100.8	−94.0	−95.1	−93.2
	(−135.7)	(−85.9)			(−108.3)	(−100.0)	(−103.1)	(−100.4)
GIAO/TZ2P	−141.6	−95.6	−131.6	−98.8	−108.9	−102.3	−101.8	−99.8
	(−141.0)	(−94.3)			(−115.5)	(−107.6)	(−109.4)	(−106.8)

[a] Distances given in the first row correspond to *r*N···N separations (see the text). [b] Values in parentheses pertain to relaxed geometries.

TABLE 2: Chemical Shift Anisotropies of the H3 Atom of Thymine as Predicted Using Different Approaches[a,b]

	2.65 Å		2.79 Å		3.50 Å		∞	
approach	CSA_a [ppm]	Γ [ppm]	CSA_a [ppm]	Γ [ppm]	CSA_a [ppm]	Γ [ppm]	CSA_a [ppm]	Γ [ppm]
IGLO/III	30.09	27.34	25.50	23.07	13.03	11.55	5.40	4.72
	(30.63)	(27.97)			(12.29)	(10.28)	(4.84)	(4.08)
IGLO/JMN2	29.77	27.02	25.17	22.72	12.68	11.15	5.52	4.94
	(30.31)	(27.65)			(11.96)	(9.89)	(4.53)	(3.81)
GIAO/TZ2P	29.64	26.47	25.11	22.22	12.95	10.93	5.29	4.20
	(30.19)	(26.64)			(12.21)	(9.57)	(4.72)	(3.54)

[a] Distances given in the first row correspond to *r*N···N separations (see the text). [b] Values in parentheses pertain to relaxed geometries.

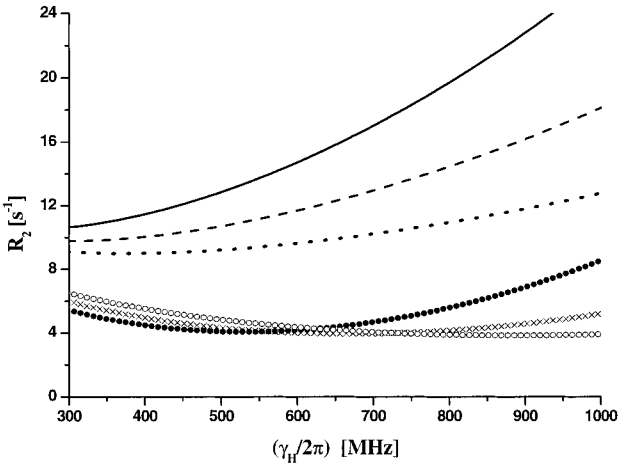

Figure 3. Transverse relaxation rate dependence on the spectrometer strength theoretically predicted for the imino proton in the guanine−cytosine base pair. Straight lines: single quantum coherence for a molecule with short (solid line; *r*N···N = 2.65 Å), typical (dashed line; *r*N···N = 2.89 Å), and long (dotted line; *r*N···N = 3.25 Å) hydrogen bonds. Symbols: the slowly relaxing (TROSY) component of the HN doublet for *r*N···N values of 2.65 Å (solid circles), 2.89 Å (crosses), and 3.25 Å (open circles). See the text for details of simulations.

shown in Table 1 (N3 atom of thymine) and Table 2 (H3 atom of thymine). Only data directly involved in analyzing NMR relaxation, i.e., CSA_a and Γ, are given for brevity. It is readily seen that an extension of the basis set from the IGLO−III to JMN2 causes negligible changes in relaxation parameters. All IGLO/III θ angles are converged up to 1°, while principal elements within 1 and 2 ppm for ^{1}H and ^{15}N shielding tensors, respectively, with respect to values obtained with JMN2 basis set (see Supporting Information, Tables 2S−5S). Hence, the IGLO−III basis set can be considered saturated for calculations of relaxation parameters in the SOS-DFPT-IGLO framework.

The differences between GIAO and IGLO results are also marginal. From a detailed analysis (Tables 2S−5S) of predicted tensors, only one systematic difference emerges, i.e., the overestimation of θ angles (up to 1.9° and 2.6° for ^{1}H and ^{15}N, respectively) by IGLO/III relative to GIAO/TZ2P. From a practical viewpoint, however, only the trends in changes of relaxation rates with changing hydrogen bonding are important. In this respect, the results of SOS-DFPT-IGLO and B3LYP-GIAO approaches are virtually identical (see Tables 1 and 2 and also Table 11). For example, although absolute values of ^{15}N CSA_a and Γ are higher by ca. 10 ppm when calculated using GIAO/TZ2P compared to using IGLO/III, the differences between structures with various *r*N···N's calculated using these methods agree to within 2 ppm (Table 1).

Parenthesized in Tables 1 and 2 are also given the IGLO/III, IGLO/JMN2, and GIAO/TZ2P values of CSA_a and Γ for the AT pair obtained for structures with internal coordinates other than *r*N···N relaxed. The B3LYP/6-311G approach, which was employed for partial optimizations, is expected to overestimate the deformation of hydrogen-bonded bases upon complexation with respect to more demanding (MBPT(2) BSSE-corrected) techniques.[19,22] In this context, changes in CSA_a and Γ due to relaxation of geometry can safely be neglected.

The CP technique, which was adopted here to study the basis set extension effects, has been successfully employed for NMR parameters of smaller systems.[46] In Table 3, σ_{iso}, σ_{ii}, and the smallest of θ angles are presented for thymine with dummy atoms in positions corresponding to adenine with *r*N···N = 2.65 Å and for isolated thymine. Imino group nuclei are practically unaffected by BSSE at this rather close distance. Consequently, the CP procedure was not further applied, and BSSE-uncorrected values are given in Tables 4−10. However, if ^{17}O shielding tensor elements were of interest, the basis set extension effects might complicate their analysis. This can be seen from results for the O4 of thymine, which lies only 2.75 Å from the amino nitrogen of adenine (Table 3).

Imino Nitrogens. In Tables 4−6, chemical shielding data for N3(T), N3(U), and N1(G) hydrogen-bonded nuclei are presented together with values for these atoms in isolated bases. First, the trends, which are common to all imino nitrogens of the Watson−Crick base pairs, in changes of parameters describing ^{15}N shielding tensor upon modification of *r*N···N will be analyzed.

Chemical shifts of imino nitrogens increase with increasing hydrogen bonding (i.e., with shortening *r*N···N separations). Theoretical predictions of this tendency together with quoting relevant experimental evidence were most recently given in refs 47 (for the AT and AU base pairing) and 7 (for the GC pair). Also, the values of principal elements of all imino ^{15}N shielding tensors change in the systematic way; i.e., σ_{11} and σ_{22} decrease,

TABLE 3: Assessment of Basis Set Extension Effects on the Chemical Shielding Tensors of Selected Nuclei in the Adenine−Thymine Base Pair[a,b]

atom	σ_{iso} [ppm]	σ_{11} [ppm]	σ_{22} [ppm]	σ_{33} [ppm]	θ [°]
N3	75.099	12.797	105.357	107.142	6.69
	(75.023)	(12.536)	(105.172)	(107.362)	(6.76)
H3	22.466	19.394	22.385	25.620	3.21
	(22.500)	(19.431)	(22.428)	(25.640)	(3.23)
O4	−112.484	−435.121	−196.808	294.478	10.45
	(−108.249)	(−426.934)	(−193.559)	(295.746)	(10.55)

[a] Results for thymine nuclei obtained with and without (in parentheses) the presence of basis functions in positions of adenine atoms. [b] σ_{ii}'s are the principal values of the shielding tensor, σ_{iso} is their average, and θ is the smallest of the angles between the *i*-th shielding component of respective shielding tensor in its principal axis system and the corresponding bond vector.

TABLE 4: Chemical Shielding Data of the N3 Atom of Thymine[a,b]

rN···N [Å]	δ [ppm]	σ_{11} [ppm]	σ_{22} [ppm]	σ_{33} [ppm]	θ_1 [°]	θ_2 [°]	θ_3 [°]	$\Delta\sigma$ [ppm]	$\Delta\eta$	CSA$_a$ [ppm]	Γ [ppm]
2.65	185.2	−3.8	37.1	146.2	23.4	113.4	89.9	−95.5	1.71	−134.3	−85.8
2.75	182.4	−1.1	46.9	142.1	18.6	108.5	90.0	−95.6	1.50	−126.3	−88.3
2.79	*181.5*	*−0.2*	*50.2*	*140.7*	*17.3*	*107.3*	*90.0*	*−95.7*	*1.42*	*−123.6*	*−89.0*
2.85	180.2	1.0	55.5	138.2	15.6	105.6	90.0	−95.8	1.29	−119.6	−89.9
2.95	178.4	2.7	63.0	134.4	13.6	103.6	90.0	−96.0	1.11	−114.2	−91.0
3.05	177.0	4.0	69.5	130.9	12.2	102.2	90.0	−96.2	0.96	−109.9	−91.8
3.25	175.0	6.0	79.4	124.8	10.4	100.4	90.0	−96.0	0.71	−103.8	−92.5
3.50	173.5	7.9	88.0	119.0	9.1	99.1	90.0	−95.6	0.49	−99.3	−92.6
∞	169.9	12.7	105.2	107.5	6.8	96.8	90.0	−93.7	0.04	−93.7	−91.7

[a] The rN···N separation is defined in the text, δ's the isotropic ^{15}N chemical shifts obtained by subtracting the isotropic shieldings from σ_{iso}= 245.07 ppm of ^{15}N in liquid NH_3, which is an experimental value from the literature,[57] σ_{ii}'s are the principal values of the shielding tensor, and θ_i's are the angles between the *i*-th shielding component and the N3(T)−H3(T) internuclear vector; parameters $\Delta\sigma$, $\Delta\eta$, CSA$_a$, and Γ were calculated using eqs 2a, 3a, 4, and 6, respectively. [b] Italicized are the values for the equilibrium geometry at the B3LYP/6-311G level.

TABLE 5: Chemical Shielding Data of the N3 Atom of Uracil[a,b]

rN···N [Å]	δ [ppm]	σ_{11} [ppm]	σ_{22} [ppm]	σ_{33} [ppm]	θ_1 [°]	θ_2 [°]	θ_3 [°]	$\Delta\sigma$ [ppm]	$\Delta\eta$	CSA$_a$ [ppm]	Γ [ppm]
2.65	187.7	−7.4	34.9	144.6	25.4	115.4	90.0	−97.1	1.70	−135.9	−85.4
2.75	184.7	−4.0	44.6	140.7	20.4	110.4	90.0	−96.7	1.49	−127.6	−87.8
2.78	*183.8*	*−3.1*	*47.6*	*139.4*	*19.1*	*109.1*	*90.0*	*−96.6*	*1.43*	*−125.1*	*−88.4*
2.85	182.3	−1.7	53.2	136.8	17.1	107.1	90.0	−96.7	1.30	−120.8	−89.6
2.95	180.6	0.0	60.7	133.0	14.8	104.8	89.9	−96.9	1.12	−115.4	−90.9
3.05	179.1	1.5	66.9	129.6	13.3	103.3	89.6	−96.7	0.97	−110.9	−91.5
3.25	177.0	3.9	77.0	123.5	11.4	101.4	90.0	−96.4	0.72	−104.5	−92.1
3.50	175.3	5.8	85.6	117.8	10.0	100.0	90.0	−95.9	0.50	−99.9	−92.3
∞	171.7	10.7	103.0	106.4	7.5	97.5	89.9	−94.0	0.06	−94.1	−91.7

[a] The rN···N separation is defined in the text, δ's are the isotropic ^{15}N chemical shifts obtained by subtracting the isotropic shieldings from σ_{iso} = 245.07 ppm for ^{15}N in liquid NH_3, which is an experimental value from the literature,[57] σ_{ii}'s are the principal values of the shielding tensor, and θ_i's are the angles between the *i*-th shielding component and the N3(U)−H3(U) internuclear vector; parameters $\Delta\sigma$, $\Delta\eta$, CSA$_a$, and Γ were calculated using eqs 2a, 3a, 4, and 6, respectively. [b] Italicized are the values for the equilibrium geometry at the B3LYP/6-311G level.

TABLE 6: Chemical Shielding Data of the N1 Atom of Guanine[a,b]

rN···N [Å]	δ [ppm]	σ_{11} [ppm]	σ_{22} [ppm]	σ_{33} [ppm]	θ_1 [°]	θ_2 [°]	θ_3 [°]	$\Delta\sigma$ [ppm]	$\Delta\eta$	CSA$_a$ [ppm]	Γ [ppm]
2.65	163.5	1.4	73.4	170.1	24.5	114.5	90.0	−120.4	1.20	−146.6	−101.7
2.75	161.5	3.4	81.7	165.7	21.4	111.4	90.0	−120.3	1.05	−140.6	−104.7
2.80	160.7	4.2	85.5	163.5	20.2	110.2	90.0	−120.3	0.97	−138.0	−105.8
2.85	160.0	4.9	89.0	161.4	19.1	109.1	90.0	−120.2	0.90	−135.6	−106.7
2.89	*159.5*	*5.5*	*91.7*	*159.7*	*18.4*	*108.4*	*90.0*	*−120.2*	*0.85*	*−133.8*	*−107.4*
2.95	158.9	6.1	95.3	157.3	17.4	107.4	90.0	−120.1	0.77	−131.6	−108.1
3.05	158.0	7.2	100.7	153.4	16.1	106.1	90.0	−119.8	0.66	−128.2	−109.0
3.25	157.0	9.0	109.2	146.1	14.3	104.3	90.0	−118.7	0.47	−122.9	−109.5
3.50	156.3	10.3	116.6	139.4	12.9	102.9	90.0	−117.7	0.29	−119.3	−109.7
∞	154.0	16.1	125.1	132.1	9.4	90.0	99.4	−112.5	0.09	−112.6	−107.8

[a] The rN···N separation is defined in the text, δ's are the isotropic ^{15}N chemical shifts obtained by subtracting the isotropic shieldings from σ_{iso} = 245.07 ppm of ^{15}N in liquid NH_3, which is an experimental value from the literature,[57] σ_{ii}'s are the principal values of the shielding tensor, and θ_i's are the angles between the *i*-th shielding component and the N1(G)−H1(G) internuclear vector; parameters $\Delta\sigma$, $\Delta\eta$, CSA$_a$, and Γ were calculated using eqs 2a, 3a, 4, and 6, respectively. [b] Italicized are the values for the equilibrium geometry at the B3LYP/6-311G level.

and σ_{33} increases with shortening lengths of the hydrogen bonds. The most sensitive is the σ_{22} principal value. These results are in agreement with an extensive study of Hu et al.,[5] where intermolecular effects on nitrogen shift tensors in nucleic acid bases were determined. To facilitate a comparison, the summary of tendencies in σ_{ii} and δ is given in Table 7 in terms of the differences between corresponding parameter in the equilibrium rN···N distance and in the isolated base.

Parameter $\Delta\sigma$ is predicted to be negligibly affected by hydrogen bonding. Qualitatively, this can be understood considering the above-mentioned trends in σ_{ii}. σ_{11} tends to decrease the value of $\Delta\sigma$ with decreasing rN···N. On the other hand,

TABLE 7: Changes in Shielding Parameters Due to the Formation of a Hydrogen-Bonded Base Pair[a,b]

base pair	imino ^{15}N				imino ^{1}H			
	$\Delta(\sigma_{11})$	$\Delta(\sigma_{22})$	$\Delta(\sigma_{33})$	$\Delta(\delta)$	$\Delta(\sigma_{11})$	$\Delta(\sigma_{22})$	$\Delta(\sigma_{33})$	$\Delta(\delta)$
AT	−12.9	−55.0	33.2	11.6	−19.3	−9.8	3.9	8.3
AU	−13.8	−55.4	33.0	12.1	−19.5	−9.9	3.8	8.5
GC	−10.6	−33.4	27.6	5.5	−15.6	−7.5	3.2	6.6

[a] The differences, Δ, between the value of given shielding parameter at the equilibrium *r*N···N (see the text) and in the isolated base are shown. [b] All values are in ppm.

σ_{22} and σ_{33} tend to cancel each other out. However, changes in σ_{22} are more pronounced than in σ_{33}, and they go in the same direction as that for σ_{11} but have the opposite sign in formula 3a. The asymmetry factor of the imino ^{15}N nuclei was recently described to increase with shortening the hydrogen bond length in the GC pair.[7] The same tendency comes out from the present work for all three Watson−Crick base pairs. With practically constant $\Delta\sigma$, deviations from axial symmetry of imino ^{15}N shielding tensors can thus be considered to be the source of the site-specific variations in the CSA_a values (see eq 4). The implications for motional models of biological macromolecules resulting from a neglect of these variations were detailed elsewhere.[48,7]

Not only $\Delta\eta$'s but also θ_1's were found to increase substantially with decreasing *r*N···N values in the GC pair.[7] Again, this trend remains valid for the AT and AU pairs as well. Consequently, when hydrogen bonds are shorter, $P_2(\cos\theta_1)$ terms diminish, which dampens the accompanying decrease in σ_{11} (see above). Values of $P_2(\cos\theta_2)$ become less negative for smaller *r*N···N values (Tables 4−6), thus rendering smaller decrease in the Γ values. On the other hand, θ_3 also has a constant value of 90° for short hydrogen bonds, which leads to more negative ($-\sigma_{33}/2$) contributions to Γ because σ_{33} increases with hydrogen bonding. As a result, the value of Γ changes moderately with *r*N···N. The consequences of this observation for NMR investigation of molecular dynamics were discussed in the communication.[7]

TABLE 8: Chemical Shielding Data of the H3 Atom of Thymine[a,b]

*r*N···N [Å]	δ [ppm]	σ_{11} [ppm]	σ_{22} [ppm]	σ_{33} [ppm]	θ_1 [°]	θ_2 [°]	θ_3 [°]	$\Delta\sigma$ [ppm]	$\Delta\eta$	CSA_a [ppm]	Γ [ppm]
2.65	19.6	−4.6	9.9	30.0	89.9	91.4	1.3	27.4	0.79	30.1	27.4
2.75	17.8	−1.0	12.0	29.6	89.9	91.5	1.5	24.1	0.81	26.6	24.1
2.79	*17.2*	*0.1*	*12.6*	*29.5*	*90.0*	*91.6*	*1.5*	*23.1*	*0.81*	*25.5*	*23.1*
2.85	16.4	2.0	13.7	29.3	89.9	91.6	1.7	21.4	0.82	23.7	21.4
2.95	15.2	4.5	15.2	28.9	89.9	91.8	1.7	19.1	0.84	21.3	19.1
3.05	14.1	6.6	16.4	28.7	89.9	91.9	1.9	17.2	0.85	19.2	17.2
3.25	12.6	9.9	18.2	28.2	90.0	92.0	2.0	14.1	0.88	15.9	14.1
3.50	11.3	12.7	19.6	27.7	89.9	92.1	2.0	11.6	0.90	13.0	11.6
∞	8.9	19.4	22.4	25.6	89.9	93.2	3.2	4.7	0.95	5.4	4.7

[a] The *r*N···N separation is defined in the text, δ's are the isotropic ^{1}H chemical shifts obtained by subtracting the isotropic shieldings from σ_{iso} = 31.339 ppm for protons in TMS calculated using the same approach as for H3(T), σ_{ii}'s are the principal values of the shielding tensor, and θ_i's are the angles between the *i*-th shielding component and the H3(T)−N3(T) internuclear vector; parameters $\Delta\sigma$, $\Delta\eta$, CSA_a, and Γ were calculated using eqs 2b, 3b, 4, and 6, respectively. [b] Italicized are the values for the equilibrium geometry at the B3LYP/6-311G level.

TABLE 9: Chemical Shielding Data of the H3 Atom of Uracil[a,b]

*r*N···N [Å]	δ [ppm]	σ_{11} [ppm]	σ_{22} [ppm]	σ_{33} [ppm]	θ_1 [°]	θ_2 [°]	θ_3 [°]	$\Delta\sigma$ [ppm]	$\Delta\eta$	CSA_a [ppm]	Γ [ppm]
2.65	19.5	−4.2	9.8	29.9	90.0	92.1	2.1	27.1	0.77	29.7	27.0
2.75	17.8	−0.7	11.8	29.5	90.0	92.2	2.2	23.9	0.79	26.2	23.8
2.78	*17.3*	*0.4*	*12.4*	*29.3*	*89.9*	*92.3*	*2.3*	*22.9*	*0.79*	*25.2*	*22.9*
2.85	16.3	2.3	13.6	29.1	90.0	92.4	2.4	21.1	0.80	23.3	21.1
2.95	15.1	4.9	15.0	28.8	90.0	92.6	2.5	18.8	0.81	20.8	18.8
3.05	14.1	7.0	16.2	28.5	89.9	92.8	2.8	16.9	0.82	18.7	16.8
3.25	12.5	10.3	18.1	28.0	89.8	93.1	3.1	13.8	0.84	15.4	13.8
3.50	11.3	13.1	19.5	27.6	89.9	93.3	3.2	11.3	0.85	12.5	11.2
∞	8.8	19.9	22.3	25.5	89.6	90.5	0.6	4.4	0.83	4.9	4.4

[a] The *r*N···N separation is defined in the text, δ's are the isotropic ^{1}H chemical shifts obtained by subtracting the isotropic shieldings from σ_{iso} = 31.339 ppm for protons in TMS calculated using the same approach as for H3(U), σ_{ii} 'sare the principal values of the shielding tensor, and θ_i's are the angles between the *i*-th shielding component and the H3(U)−N3(U) internuclear vector; parameters $\Delta\sigma$, $\Delta\eta$, CSA_a, and Γ were calculated using eqs 2b, 3b, 4, and 6, respectively. [b] Italicized are the values for the equilibrium geometry at the B3LYP/6-311G level.

TABLE 10: Chemical Shielding Data of the H1 Atom of Guanine[a,b]

*r*N···N [Å]	δ [ppm]	σ_{11} [ppm]	σ_{22} [ppm]	σ_{33} [ppm]	θ_1 [°]	θ_2 [°]	θ_3 [°]	$\Delta\sigma$ [ppm]	$\Delta\eta$	CSA_a [ppm]	Γ [ppm]
2.65	18.2	−3.7	12.8	30.5	90.0	91.7	1.6	26.0	0.95	29.6	26.0
2.75	16.4	−0.2	14.9	30.0	89.9	91.8	1.8	22.7	1.00	26.2	22.7
2.80	15.7	1.3	15.8	29.8	90.0	91.8	1.8	21.3	1.02	24.7	21.3
2.85	15.0	2.7	16.6	29.6	90.0	91.9	1.8	20.0	1.05	23.4	20.0
2.89	*14.5*	*3.7*	*17.2*	*29.5*	*90.0*	*91.9*	*1.9*	*19.0*	*1.06*	*22.3*	*19.0*
2.95	13.9	5.1	18.0	29.3	90.0	92.0	2.0	17.7	1.09	21.0	17.7
3.05	12.9	7.1	19.2	29.0	89.9	92.2	2.2	15.9	1.14	19.0	15.8
3.25	11.4	10.3	20.9	28.6	89.9	92.8	2.8	13.0	1.22	15.9	13.0
3.50	10.3	12.9	22.1	28.2	89.9	93.7	3.8	10.7	1.30	13.3	10.6
∞	7.9	19.3	24.7	26.3	89.9	104.7	14.7	4.3	1.86	6.3	4.2

[a] The *r*N···N separation is defined in the text, δ's are the isotropic ^{1}H chemical shifts obtained by subtracting the isotropic shieldings from σ_{iso} = 31.339 ppm for protons in TMS calculated using the same approach as for H1(G), σ_{ii}'s are the principal values of the shielding tensors, and θ_i's are the angles between the *i*-th shielding component and the H1(G)−N1(G) internuclear vector; parameters $\Delta\sigma$, $\Delta\eta$, CSA_a, and Γ were calculated using eqs 2b, 3b, 4, and 6, respectively. [b] Italicized are the values for the equilibrium geometry at the B3LYP/6-311G level.

Calculations with *r*N···N = 2.65, 2.75, 2.85, 2.95, 3.05, 3.25, and 3.50 Å and for the corresponding equilibrium separation were carried out for each base pair, which enables an immediate comparison of magnitudes of shielding parameters between respective hydrogen-bonded bases. The structure difference between uracil and thymine, i.e., the presence of the methyl group in position 5 of the latter, causes rather small differences in the ^{15}N shielding data of corresponding N3 nuclei (cf. Tables 4 and 5 and also Table 7). This is not surprising in light of a very small difference of only 2 and 1 ppm between the chemical shifts of N3(T) and N3(U) atoms in the liquid[49] and the solid states,[5] respectively. In both experiments, the chemical shift of N3(U) was reported to be higher than that for N3(T). Interestingly, this tendency holds for all *r*N···N distances studied here. Thus, the N3(U) and N3(T) shielding data will be collectively referred to as N3(pyrimidine) in the following.

The principal elements of ^{15}N shielding tensors of the N1(G) atoms for respective *r*N···N separations are markedly higher than their N3(pyrimidine) counterparts. This causes that CSA_a values for N1(G) are ~10 ppm higher than the corresponding N3(pyrimidine) values. Moreover, for given *r*N···N, the deflections of both σ_{11} and σ_{22} principal components from the imino ^{15}N−^{1}H bond vector are slightly smaller for N1(G), which leads to even higher (ca. 15 ppm) differences in the values of Γ between N1(G) and N3(pyrimidine). For the accurate extraction of motional parameters from NMR relaxation studies, however, the base-to-base variation in CSA_a and/or Γ is essential. Namely, the smaller the variation in the chemical shift anisotropy contribution to relaxation, the smaller errors are introduced into molecular dynamics by taking uniform CSA_a and/or Γ values for all residues in the molecule of nucleic acid.[7] In this respect, the results for N1(G) and N3(pyrimidine) are quite similar. For example, the differences in the CSA_a between the shortest (2.65 Å) and equilibrium *r*N···N are 10.8 and 12.8 ppm for the AU and the GC pair, respectively, while the differences in the Γ values are considerably lower (3.0 and 5.7 ppm, respectively). The variation in the CSA_a between the equilibrium *r*N···N separation and a very long hydrogen bond of 3.25 Å is predicted to be 20.6 and 10.9 ppm for the AU and the GC pair, respectively. The corresponding changes in the values of Γ are substantially smaller (3.7 and 2.1 ppm, respectively). As a consequence, the conclusion derived for the GC residues[7] that the parameters of molecular motion based on cross-correlation rates would provide more accurate values than those based on auto-correlation rates is valid for imino ^{15}N nuclei in all Watson−Crick base pairs.

Imino Protons. The chemical shielding data for H3(T), H3(U), and H1(G) nuclei are collected in Tables 8−10. In nucleic acids, imino protons are exchangeable, with exchange times ranging from days to less than 1 ms.[50] Hence, a large number of factors govern the positions of their resonances; special methods have been developed for their assignment.[51] Obviously, a quantitative agreement of the results for base pairs in vacuo with experimental values obtained for residues in biomolecules can hardly be expected. The discrepancies are clearly visible from a comparison of the computed chemical shifts with typical values found in nucleic acids. The latter normally lie in the interval between 10 and 15 ppm[52] and thus are a few parts per million lower than the calculated data. Nevertheless, the trend in changes of the imino ^{1}H chemical shifts with hydrogen bonding is qualitatively reproduced: the calculated chemical shifts of imino protons in all Watson−Crick base pairs decrease with increasing *r*N···N separations, which agrees with experimental observations. For example, in the short spliced leader RNA sequence,[53] the chemical shifts of H1(G) protons in the residues G22 and G23 located at the helix-loop junction and forming the Watson−Crick base pairs are 12.52 and 13.13 ppm, respectively, while for the G16 site in the loop region, which has a limited opportunity to create hydrogen bonds, the value of the imino ^{1}H chemical shift is 10.68 ppm. Consequently, the systematic variation found for the remaining shielding parameters of all Watson−Crick base pairs will briefly be discussed as well (Tables 8−10).

Notably, the values of σ_{11} and σ_{22} imino ^{1}H shielding tensor components change dramatically in response to hydrogen bonding. They both decrease with shortening *r*N···N separation. On the other hand, σ_{33} principal elements are much less affected, their values being elevated about 2 ppm for shorter hydrogen bonds. Interestingly, in the analysis of O−H···O bonded ^{1}H shielding tensors measured in the solid state, the σ_{33} component has been found to be independent of the degree of hydrogen bonding within experimental errors; anisotropies of up to 37.0 ppm have been considered.[54] On the basis of present ab initio data, one is tempted to speculate that an experimental study of the imino ^{1}H CSA would lead to a similar conclusion.

Parameter $\Delta\sigma$ is changing substantially with varying *r*N···N distance. As was the case with the (practically constant) $\Delta\sigma$ of imino ^{15}N shielding tensors, the trend can be explained in terms of variations in σ_{ii} described above. For short *r*N···N, the near-cancellation of σ_{11} (which becomes negative) and σ_{22} occurs. Consequently, the σ_{33} component dominates the $\Delta\sigma$ value. For long (or absent) hydrogen bonds, the magnitudes of σ_{11} and σ_{22} are comparable to that of σ_{33}. This brings about small values of $\Delta\sigma$ (eq 2b). As has been described for the GC pair recently,[7] the imino ^{1}H shielding tensor is nonsymmetric for any length of the hydrogen bond, with the asymmetry factor only moderately affected by variation in *r*N···N. Nonetheless, CSA_a values are predicted to vary dramatically with *r*N···N due to the above-mentioned changes in $\Delta\sigma$.

The principal axes of imino ^{1}H shielding tensors have practically fixed orientation for the whole range of hydrogen bond lengths. Moreover, the direction of the σ_{33} principal component departs negligibly from collinearity with the imino ^{1}H−^{15}N internuclear vector. As a result, the values of the cross-correlation parameter Γ approach self-relaxation data, and consequently, they undergo significant changes with varying *r*N···N as well.

Calculations for identical *r*N···N separations do not reveal any significant differences between shielding parameters of the H3(T) and H3(U) protons (Tables 7−10). A rather interesting trend emerges from a comparison of H3(pyrimidine) (i.e., H3(T) or H3(U)) versus H1(G) shielding tensors. The principal values of the latter are higher, which immediately leads to a prediction of lower chemical shifts of guanine imino protons compared to their pyrimidine counterparts. In nucleic acids, this trend in chemical shifts can be experimentally observed in the majority of cases. For example, in the above-mentioned RNA sequence,[53] the chemical shifts of H3(U) protons in the loop residues U8 and U9 are 14.34 and 13.15 ppm, respectively, as compared to 10.68 ppm of H1(G) in the G16 (see above). Both CSA_a and Γ have rather similar magnitudes for the H3-(pyrimidine) and H1(G) imino ^{1}H nuclei. The inspection of respective contributions to R_2^{TR} and R_2^{SQ} (data not shown) indicates that small differences in relaxation behavior (vide infra) between the H1(G) and H3(T) atoms stem mainly from the dipolar terms.

Relaxation Rates. Straightforward simulations of the dependence on the static magnetic field of spin−spin relaxation rates

TABLE 11: Spin−Spin Relaxation Rates for the Slowly Relaxing Component of the Doublet, R_2^{TR}, and for Single Quantum Coherence, R_2^{SQ}, of the Imino Proton in the Adenine−Thymine Pair at External Fields of 500 and 900 MHz[a,b]

	500 MHz		900 MHz	
*r*N···N [Å]	R_2^{TR} [s^{-1}]	R_2^{SQ} [s^{-1}]	R_2^{TR} [s^{-1}]	R_2^{SQ} [s^{-1}]
2.65	3.00 (3.17)	11.75 (11.60)	6.19 (6.25)	22.12 (21.63)
2.79	2.85 (3.07)	10.23 (10.13)	4.14 (4.36)	17.58 (17.24)

[a] Calculated employing IGLO/III and GIAO/TZ2P (in parentheses) chemical shift anisotropies and using a simplified model of relaxation described in the text. [b] The *r*N···N separation is defined in the text.

for single quantum coherence and for the slowly relaxing component of the doublet of imino protons were carried out (see Theory and Computations for details). The resulting curves for the AT and the GC pairs with short (2.65 Å), equilibrium (2.787 and 2.891 Å, respectively), and very long (3.25 Å) *r*N···N separations are shown in Figures 2 and 3, respectively.

The $R_2(B_0)$ dependence was found to be insensitive to the variation in the generalized order parameter. Consequently, calculations with S^2 set to 0.75, i.e., for model of a moderately flexible molecule, are presented. IGLO/III chemical shift anisotropies were used throughout.

SQ relaxation rates grow rather quickly with the increasing magnetic field for residues with shorter hydrogen bonds. Obviously, this is caused by large CSA_a values for short *r*N···N distances and the dependence of the CSA autocorrelation on the square of B_0 (cf. eqs 11 and 12). For long hydrogen bonds, the increase is not as dramatic (dotted curves in Figures 2 and 3). Due to the cross-correlated cross-relaxation of the ^{1}H−^{15}N spin pair (eq 13), the relaxation rate reduction occurs in the alternative TROSY[8] experiment. Unlike in the case of imino ^{15}N nuclei,[7] the effect of cross-correlation on the imino proton is predicted to be significant at currently available field strengths also for residues with longer hydrogen bonds. According to the simulations described above, TROSY optima (i.e., points with vanishing dR_2^{TR}/dB_0) for the AT pair are at 12.0, 13.9, and 21.2 T for *r*N···N's of 2.65, 2.787, and 3.25 Å, respectively. For the GC pair, they lie at 12.5, 15.7, and 20.8 T for *r*N···N's of 2.65, 2.891, and 3.25 Å, respectively.

The sensitivity increase of the TROSY measurement over SQ can be anticipated from Table 11, where relaxation rates at 500 and 900 MHz are shown. The AT pairs with short (2.65 Å) and equilibrium *r*N···N distances are investigated. A significant decrease in R_2^{TR} relative to R_2^{SQ} is predicted already at 500 MHz, which can be employed mainly in minimizing the signal loss due to relaxation in through-bond experiments on nucleic acids.[55] Clearly, the differences $R_2^{TR}-R_2^{SQ}$ are elevated for shorter hydrogen bonds and for higher B_0. However, the R_2 values in Table 11 should be interpreted in qualitative terms only. They were computed for an assessment of possible sensitivity gain of TROSY over SQ experiment, not as absolute values. Their calculations are based on several simplified assumptions concerning mainly

(i) the neglect of chemical exchange contributions to NMR relaxation,

(ii) the application of uniform one-bond direct dipolar couplings (eq 9) for all residues (as a result of using the constant r_{NH} distance for the given base pair), and

(iii) the neglect of dipolar effects of distant protons separated more than 3.0 Å from the imino proton.

However, chemical exchange effects (assumption i) are likely to influence both transverse relaxation rates by approximately the same amount; assumptions ii and iii do not constitute a problem when the difference in relaxation rates is of interest, since dipolar contributions to R_2^{TR} and R_2^{SQ} are identical (cf. eqs 7 and 8).

Parenthesized in Table 11 are R_2 data computed for GIAO/TZ2P shielding tensors. As could be anticipated from Tables 1 and 2, predicted relaxation rates and $R_2^{TR} - R_2^{SQ}$ differences are fairly similar to values obtained using IGLO/III chemical shift anisotropies.

Conclusions

A systematic ab initio investigation with the inclusion of electron correlation of chemical shielding parameters of the imino ^{15}N and ^{1}H nuclei in hydrogen-bonded Watson−Crick base pairs has been presented. The results strongly suggest that the significant variation in parameters governing the CSA mechanism of NMR relaxation can be expected along the backbone of a DNA or RNA molecule. This should be taken into consideration in residue-specific analyses of internal mobility in nucleic acids. The findings of the present study will be summarized in the order of the questions posed in the Introduction.

(1) The SOS-DFPT-IGLO and the B3LYP-GIAO methods, when applied with large basis sets, predict very similar values of shielding parameters. The SOS-DFPT-IGLO computations require much smaller investment of the CPU time and thus are to be preferred for (fragments of) nucleic acids.

(ii) Basis set extension effects on the SOS-DFPT-IGLO shielding data obtained with the IGLO−III basis set of Kutzelnigg et al. of imino nuclei can safely be neglected.

(iii) The relaxation of the base pair geometry does not significantly affect the changes of chemical shift anisotropies with varying hydrogen bond length. However, a noticeable effect on the values of dipolar terms (through effective bond lengths) may be expected.[56]

(iv) The structure difference between uracil and thymine does not translate into any substantial differences in shielding data of their hydrogen-bonded imino atoms.

(v) The direction of the least shielded component of the imino ^{15}N chemical shielding tensor is tilted from the imino bond vector[7] at roughly the same value for all Watson−Crick base pairs. However, in the investigated range of separations between bases, principal values of this tensor in pyrimidines are consistenly higher than those in their guanine counterparts. Nevertheless, the predicted changes with hydrogen bonding of auto- and cross-correlation CSA parameters are quite similar for guanine and pyrimidine sites. This holds for imino protons as well.

(vi) According to simulations based on ab initio data, the use of the TROSY principle in NMR studies of imino protons both in RNA and DNA promises an efficient suppression of their transverse relaxation at currently available spectrometers. Thus, an improved sensitivity of heteronuclear experiments involving imino protons may be achieved.

Acknowledgment. I would like to thank Prof. V. Sklenář and Dr. R. Fiala for stimulating discussions on NMR relaxation and for critically reading the manuscript and Dr. J. Šponer for his assistance in optimizing the geometries of base pairs. This research has been supported by the Grant Agency of the Czech Republic (Grants 203/99/0311 and 203/99/0576) and by the Ministry of Education of the Czech Republic (Grants VS96095 and J07/98:143100005). Time allocation in the Czech Academic Supercomputer Centre is gratefully acknowledged.

Supporting Information Available: B3LYP/6-311G geometries of the minimum of the AT pair and of the AT structures

with rN···N = 2.65 and 3.50 Å (Table 1S). Principal elements of the imino nitrogen and imino proton shielding tensors and corresponding θ angles predicted using IGLO/III, IGLO/JMN2, and GIAO/TZ2P approaches for different geometries of the AT pair (Tables 2S−5S). This material is available free of charge at http://pubs.acs.org.

References and Notes

(1) Palmer, A. G., III; Williams, J.; McDermott, A. *J. Phys. Chem.* **1996**, *100*, 13293.

(2) Fischer, M. W. F.; Majumdar, A.; Zuiderweg, E. P. R. *Prog. NMR Spectrosc.* **1998**, *33*, 207.

(3) Akke, M.; Fiala, R.; Jiang, F.; Patel, D.; Palmer, A. G., III *RNA* **1997**, *3*, 702.

(4) Saenger, W. *Principles of Nucleic Acid Structure*; Springer-Verlag: New York, 1983.

(5) Hu, J. Z.; Facelli, J. C.; Alderman, D. W.; Pugmire, R. J.; Grant, D. M. *J. Am. Chem. Soc.* **1998**, *120*, 9863.

(6) Sitkoff, D.; Case, D. A. **1994**, *Prog. NMR Spectrosc.* **1998**, *32*, 165.

(7) Czernek, J.; Fiala, R.; Sklenář, V. *J. Magn. Res.* **2000**, *145*, 142.

(8) Pervushin, K.; Riek, R.; Wider, G.; Wüthrich, K. *Proc. Natl. Acad. Sci. U.S.A.* **1997**, *94*, 12366.

(9) Fiala, R.; Czernek, J.; Sklenář, V. *J. Biomol. NMR* **2000**, *16*, 291.

(10) Helgaker, T.; Jaszuński, M.; Ruud, K. *Chem. Rev.* **1999**, *99*, 293.

(11) Parr, R. G.; Yang, W. *Density-Functional Theory of Atoms and Molecules*; Oxford University Press: Oxford, 1989.

(12) Cheeseman, J. R.; Trucks, G. W.; Keith, T. A.; Frish, M. J. *J. Chem. Phys.* **1996**, *104*, 5497.

(13) Malkin, V. G.; Malkina, O. L.; Casida, M. E.; Salahub, D. R. *J. Am. Chem. Soc.* **1994**, *116*, 5898.

(14) Malkin, V. G.; Malkina, O. L.; Eriksson, L. A.; Salahub, D. R. In *Theoretical and Computational Chemistry*; Seminario, J. M., Politzer, P., Eds.; Elsevier: Amsterdam, 1995; Vol. 2, p 273.

(15) Bühl, M.; Kaupp, M.; Malkina, O. L.; Malkin, V. G. *J. Comput. Chem.* **1999**, *20*, 91.

(16) Clementi E.; Corongiu G.; Chakravorty S. In *Modern Techniques in Computational Chemistry*; Clementi, E., Ed.; ESCOM: Leiden, 1990; p 343.

(17) Ernst, R. R.; Bodenhausen, G.; Wokaun, A. *Principles of NMR in One and Two Dimensions*; Clarendon Press: Oxford, 1987.

(18) Sklenář, V.; Peterson, R. D.; Rejante, M. R.; Feigon, J. *J. Am. Chem. Soc.* **1993**, *115*, 12181.

(19) Hobza, P.; Šponer, J. *Chem. Rev.* **1999**, *99*, 3247.

(20) Szabo, A.; Ostlund, N. S. *Modern Quantum Chemistry*; McGraw-Hill: New York, 1982.

(21) Santamaria, L. R.; Charro, E.; Zacarias, A.; Castro, M. *J. Comput. Chem.* **1999**, *20*, 511.

(22) Šponer, J. Personal communication.

(23) Becke, A. D. *J. Chem. Phys.* **1993**, *98*, 5648.

(24) Lee, C.; Yang, W.; Parr, R. *Phys. Rev. B* **1998**, *37*, 785.

(25) Šponer, J.; Leszczynski, J.; Hobza, P. *J. Phys. Chem.* **1996**, *100*, 1965.

(26) Frish, M. J.; Trucks, G. W.; Schlegel, H. B.; Gill, P. M. W.; Johnson, B. G.; Robb, M. A.; Cheeseman, J. R.; Keith, T.; Petersson, G. A.; Montgomery, J. A.; Raghavachari, K.; Al-Laham, M. A.; Zakrzewski, V. G.; Ortiz, J. V.; Foresman, J. B.; Cioslowski, J.; Stefanov, B. B.; Nanayakkara, A.; Challacombe, M.; Peng, C. Y.; Ayala, P. Y.; Chen, W.; Wong, M. W.; Andres, J. L.; Replongle, E. S.; Gomperts, R.; Martin, R. L.; Fox, D. J.; Binkley, J. S.; Defrees, D. J.; Baker, J.; Stewart, J. P.; Head-Gordon, M.; Gonzales, C.; Pople, J. A. *Gaussian 94*, Revision C.2; Gaussian, Inc.: Pittsburgh, PA, 1995.

(27) Dayie, K. T.; Wagner, G. *J. Am. Chem. Soc.* **1997**, *119*, 7797.

(28) Damberg, P.; Jarvet, J.; Allard, P.; Gräslund, A. *J. Biomol. NMR* **1999**, *15*, 27.

(29) Kroenke, C. D.; Loria, J. P.; Lee, L. K.; Rance, M.; Palmer, A. G., III *J. Am. Chem. Soc.* **1998**, *120*, 7905.

(30) Salahub, D. R.; Fournier, R.; Mlynarski, P.; Papai. A.; St-Amant, A.; Uskio, J. In *Density Functional Methods in Chemistry*; Labanowski, J.; Andzelm, J. W., Eds.; Springer: New York, 1991; p 77.

(31) Malkin, V. G.; Malkina, O. L.; Salahub, D. R. *MASTER−CS Program*; Universite de Montreal: Montreal, 1994.

(32) Kutzelnigg, W.; Fleischer, U.; Schindler, M. *NMR Basic Principles and Progress*, Vol. 23; Springer-Verlag: Berlin, 1990; p 165.

(33) Perdew, J. P.; Wang, Y. *Phys. Rev. B* **1992**, *45*, 13244.

(34) Perdew, J. P.; Chevary, J. A.; Vosko, S. H.; Jackson, K. A.; Pederson, M. R.; Singh, D. J.; Fiolhais, C. *Phys. Rev. B* **1992**, *46*, 6671.

(35) Boys, S. F. In *Quantum Theory of Atoms, Molecules and the Solid State*; Löwdin, P.-O., Ed.; Academic Press: New York, 1966; p 263.

(36) Ditchfield, R. *Mol. Phys.* **1974**, *27*, 789.

(37) Wolinski, K.; Hinton, J. F.; Pulay P. *J. Am. Chem. Soc.* **1990**, *112*, 8251.

(38) Schäfer, A.; Horn, H.; Ahlrichs, R. *J. Chem. Phys.* **1992**, *97*, 2571.

(39) Czernek, J.; Sklenář, V. *J. Phys. Chem. A* **1999**, *103*, 4089.

(40) Boys, S. F.; Bernardi F. *Mol. Phys.* **1970**, *19*, 553.

(41) Abragam, A. *Principles of Nuclear Magnetism*; Oxford University Press: Oxford, 1961.

(42) Lipari, G.; Szabo, A. *J. Am. Chem. Soc.* **1982**, *104*, 4546.

(43) Lipari, G.; Szabo, A. *J. Am. Chem. Soc.* **1982**, *104*, 4559.

(44) Jiang, F.; Fiala, R.; Live, D.; Kumar, R. A.; Patel, D. J. *Biochemistry* **1996**, *35*, 13250.

(45) Maple and Maple V are registered trademarks of Waterloo Maple Inc.

(46) de Dios, A. C.; Oldfield, E. *Chem. Phys. Lett.* **1993**, *205*, 108.

(47) Xu, X. P.; Au-Yeung, S. C. F. *J. Phys. Chem. B* **2000**, *104*, 5641.

(48) Fushman, D.; Cowburn, D. *J. Biomol. NMR* **1999**, *13*, 139.

(49) Witanowski, M.; Stefaniak, L.; Webb, G. A. Nitrogen NMR Spectroscopy. In *Annual Reports on NMR Specstroscopy*; Webb, G. A., Ed.; Academic Press: London, 1993; Vol. 25.

(50) Gueron, M.; Leroy J.-L. *Methods Enzymol.* **1995**, *261*, 383.

(51) Nikonowicz, E. P.; Pardi, A. *J. Mol. Biol.* **1993**, *232*, 1141.

(52) Wüthrich, K. *NMR of Proteins and Nucleic Acids*; Wiley: New York, 1986.

(53) Greenbaum, N. L.; Radhakrishnan, I.; Hirsh, D.; Patel, D. J. *J. Mol. Biol.* **1995**, *252*, 314.

(54) Berglund, B.; Vaughan, R. W. *J. Chem. Phys.* **1980**, *73*, 2037.

(55) See: Fiala, R.; Feng, J.; Patel, D. J. *J. Am. Chem. Soc.* **1996**, *118*, 689 and references therein.

(56) Case, D. A. *J. Biomol. NMR* **2000**, *15*, 95.

(57) Jameson, C. J.; de Dios, A. C. *J. Chem. Phys.* **1991**, *95*, 1069.